Progress In Electromagnetics Research M, Vol. 65, 69–78, 2018

A Comparative Study for Breast Cancer Detection by Neural Approach for Different Configurations of the Microwave Imaging System

Wassila Sekkal[1, *], Lotfi Merad[2], and Sidi M. Meriah[1]

Abstract—The study done in this paper focuses on the detection of breast cancer by neuronal approach, by rotating the transmitting antenna from 15°, 30°, 45°, 60°, 75°, to 90° relative to its initial position which is of 0° (i.e., to the opposite of the receiving antenna). We have generated our database by using a CST electromagnetic simulator for each antenna location. Then the learning and test phases of our artificial neural network (ANN) are done for seven antennae locations using two learning algorithms which are: the Scaled Conjugate Gradient Back-propagation (Trainscg) and the Gradient Descent with Momentum (Traingdm). A comparative study was conducted for all the seven cases. The results obtained are very satisfying and show that the best location of the transmitter antenna is at 60° and that the learning algorithm Trainscg gives better results than Traingdm.

1. INTRODUCTION

Breast cancer is one of the most common cancers for women. For this, detection and early intervention are one of the most important factors in improving survival rates and quality of life of people with this type of cancer, since this is the time when treatment is most effective [1]. X-ray mammography is one of the most widely used imaging methods for early detection of breast cancer. However, despite significant progress in the improvement of the mammographic technique, persistent limitations lead to high rates of false negatives [2] and high rates of false positives [3] particularly in premenopausal women where increased breast density can obscure non-palpable lesions [4]. These false-positive diagnoses result in unnecessary biopsies, causing considerable distress to the patient and unnecessary financial burden on the health service. These limitations motivate the need of other methods that can overcome such limitations in a cost-effective manner.

Microwave imaging is considered as one of the most promising approaches for the detection of breast cancer during recent years. Several works have been conducted using a numerical breast model [3, 5–7]. Microwave imaging consists of transmitting UWB signals through breast tissues and collecting received signals from different locations. When the breast is exposed to microwave radiation, the high water content of malignant breast tissues causes a more significant diffusion than healthy mammary tissues which have low water content [8]. It is reported, in the literature, that the increase in dielectric permittivity and conductivity for cancerous mammary tissues is three or more times greater than healthy tissues [5].

In this study, neural network in microwave imaging is going to be used in order to detect the presence of an eventual tumor in the breast. The proposed method has already been used in several studies [7–11]. However, the configuration of the microwave system used only one position of the transmitting antenna

Received 19 November 2017, Accepted 14 February 2018, Scheduled 1 March 2018

* Corresponding author: Wassila Sekkal (sekkalwassila@gmail.com).

[1] Laboratory of Telecommunications Tlemcen LTT, Faculty of Technology, University of Tlemcen, Algeria. [2] 2nd Cycle Department, high School of Applied Sciences, Bel-horizon, Tlemcen, Algeria.

at 0°. Different configurations of microwave imaging system by rotating the transmitter antenna from 0° to 90° with step of 15° are used to increase the recognition rate.

Our contribution consists in undertaking a comparative study for different configurations of the microwave imaging system using an artificial neural network. For this, two learning algorithms, the Scaled Conjugate Gradient Back-propagation (trainscg) and Gradient Descent with Momentum (Traingdm), are used in order to get the best configuration and best learning algorithm that gives an optimal recognition rate. It is why we position a transmitter antenna at different locations around a prototype of the breast, and then a spherical tumor is placed at arbitrary locations using an electromagnetic simulator for each antenna location. A UWB slotted antenna is used to transmit and receive ultra-wideband signals [13].

The paper is organized as follows. The following section presents steps of creating different databases for each antenna location, in order to begin the learning and testing phases of the neural network using the two algorithms. Section 3 presents the obtained results. Finally, a conclusion is given to summarize the work done in this project and also provides new perspectives for future work.

2. PROPOSED METHOD

2.1. Breast Model

In this article, the model given in [5] is taken, which has a hemispherical shape, and our study is adapted to it, as presented in Table 1 and Fig. 1.

Table 1. Model dimensions.

Model Part	Size (cm)
Breast diameter	10
Breast height	6
Skin thickness	0.2
Chest thickness	2

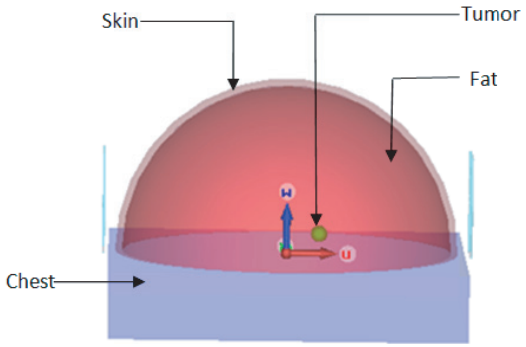

Figure 1. Breast Model with tumor under CST.

The size of the tumor has been studied several times in the literature [6, 14]. A tumor of 0.25 cm in radius is taken with the following dielectric properties as shown in Table 2, where σ is the conductivity in (Siemens/meter), and ε_r is the relative permittivity [7].

2.2. Positioning of the Antenna and Creation of Data Base

By rotating the transmitter antenna from 0°, 15°, 30°, 45°, 60°, 75° to 90° under the CST simulation software, the database is created (see Fig. 2). This study is limited to the upper right quadrant (Fig. 2), and it is the same for the other three quadrants.

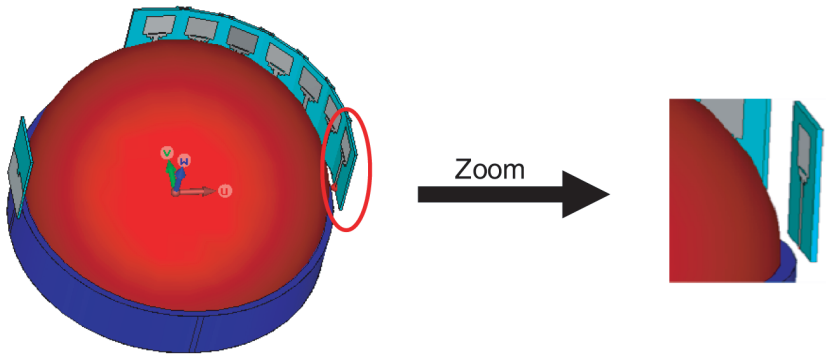

Figure 2. Different locations of the transmitting antenna.

To generate our seven databases, we proceed as follows as presented in [5]:

1) Place a pair of transmitter-receiver at opposite sides of the breast model;
2) Place a tumor at any location in the model;
3) Transmit a Gaussian pulse of a plane wave in the direction of the X and Y axes;
4) Receive the signal on the opposite side;
5) Change the tumor location and repeat steps 3 and 4.

This process of data generation has been performed for 441 different tumor locations along the X and Y axes for each position of the transmitter antenna. From this set two groups of received signals were formed as follows:

Group (1): A set of 341 signals were used for the learning of our ANN.
Group (2): A set of 100 signals were used for the testing phase of our ANN.

Table 2. Dielectric properties of the model.

	Conductivity σ (S/m)	Permittivity ε_r
Skin	1.49	37.9
Fat	0.14	5.14
Chest	1.85	53.5
Tumor	1.20	50

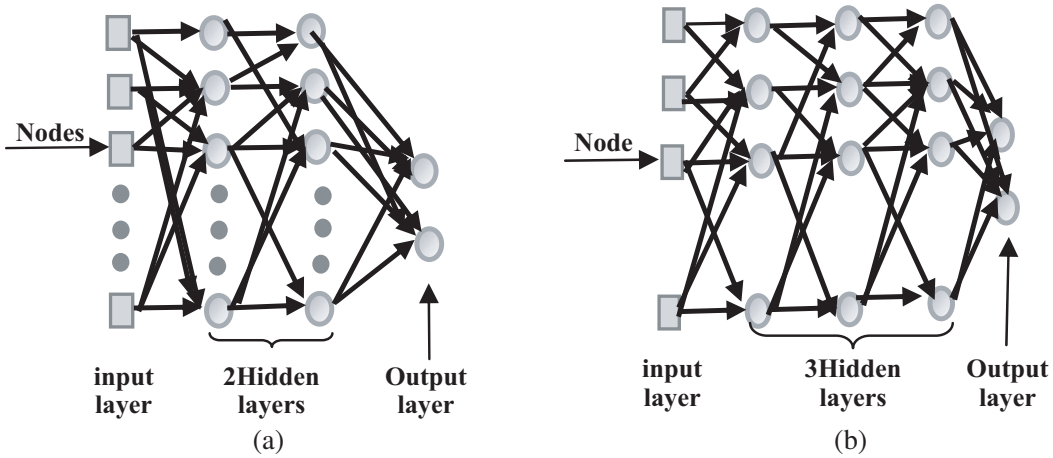

Figure 3. ANN model (a) for transmitter antenna at 0°, 15°, 30°, 45°, 60°, (b) for transmitter antenna at 75°, 90°.

2.3. Detection of the Tumor by Neural Networks

Neural networks are very performing tools for the recognition of forms and the detection of breast cancer, but the problem resides in their dimensioning because there is no theory or empirical rules that allows it. There conception is done in an experimental way. The difficulty usually arises in the choice of the number of hidden layers as well as the number of nodes in each layer. In the following section we are going to realize the design, and the learning and test phases of our artificial neural networks for each antenna location. After several tests, architectures of our neural networks retained for each antenna position are illustrated in Figs. 3(a) and (b).

The input layer contains as many neurons as the number of elements of the input vector $P(xi)$. In order to fix a sampling step of the signal, a cubic hermit interpolating polynomial is made to generate a polynomial $P(xi)$ while keeping the same pace of the signal [15]. Table 3 summarizes the number of samples obtained after interpolation with a step of 0.01 for each antenna location.

The synthetic scheme of our model is illustrated in Fig. 4.

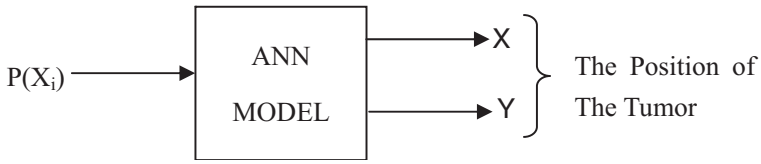

Figure 4. Representation of the ANN model synthesis.

Table 3. The number of neurons in the input layer.

Location of antenna	Time Segment	Number of neurons in the input layer
Antenna at 0°	2.8207 : 0.01 : 3.5937	78
Antenna at 15°	2.9431 : 0.01 : 3.5309	59
Antenna at 30°	2.5526 : 0.01 : 3.4988	95
Antenna at 45°	2.2019 : 0.01 : 3.5537	136
Antenna at 60°	2.4322 : 0.01 : 3.3203	89
Antenna at 75°	2.3777 : 0.01 : 3.0611	69
Antenna at 90°	2.4264 : 0.01 : 3.5911	117

Table 4 summarizes learning parameters of each neural network under MATLAB. The activation function used is a sigmoid function which has an output interval between $[-1; 1]$. Two learning algorithms are used: Scaled conjugate gradient backpropagation (Trainscg) and Gradient descent with momentum (Traingdm).

3. RESULTS

Once the learning phase was completed, the performance of our ANN was tested using group 2, shown in Figs. 5–11. In Tables 6–9 only 11 examples from group 2 are presented.

Tables 5 and 6 show the tumor detection results using the Scaled Conjugate Gradient (SCG) learning algorithm. The learning phase lasted respectively 10 hours, 3 minutes, 9 hours, 11 minutes, 2 hours, 5 hours, 5 hours for each antenna location.

Tables 7 and 8 show tumor detection results using the Gradient Descent With Momentum (GDM) learning algorithm. The learning phase lasted respectively 9 hours, 4 hours, 10 hours, 5 hours, 10 hours, 8 hours and 10 hours for each antenna location.

Table 9 summarizes the recognition rate and the relative error for each neural network studied.

Table 4. The ANN parameters for transmitter antenna at 0°, 15°, 30°, 45°, 60°, 75° and 90°.

ANN Parameters	Antenna Positions (°)						
	0	15	30	45	60	75	90
Number of nodes in input layer	78	59	95	136	89	69	117
Number of nodes in hidden layer 1	45	45	45	45	45	45	45
Number of nodes in hidden layer 2	10	10	10	10	10	10	10
Number of nodes in hidden layer 3	-	5	-	-	-	5	5
Number of nodes in output layer	02	02	02	02	02	02	02
Activation function	tansig	tansig	tansig	tansig	tansig	tansig	tansig
The learning Algorithm	trainscg/traingdm						

Table 5. Position of the tumor and the output of the ANN for a transmitter antenna at 0°, 15°, 30° and 45°.

Real position of the tumor (cm/10)		Output of the ANN (SCG)							
		Antenna at 0°		Antenna at 15°		Antenna at 30°		Antenna at 45°	
X	Y	X	Y	X	Y	X	Y	X	Y
0	0.9	0.000	0.9216	0.0024	0.9971	0.0005	0.8900	0.0000	0.90711
0.05	0.6	0.0482	0.6181	0.0422	0.6215	0.0439	0.6042	0.6715	6.2058
0.1	0.65	0.0103	0.6407	0.0987	0.6495	0.1048	0.6482	0.1224	0.6544
0.15	0.85	0.2097	0.8576	0.1362	0.9069	0.0013	0.8548	0.1903	0.8526
0.25	0.7	0.2437	0.6946	0.2532	0.6973	0.2508	0.6991	0.2519	0.6994
0.25	1	0.2483	0.9999	0.2624	0.9992	0.2476	0.9999	0.2257	0.9999
0.45	0.5	0.4449	0.5224	0.4578	0.4970	0.4500	0.4998	0.4504	0.5004
0.65	1	0.6513	1	0.6421	0.9997	0.6478	0.9999	0.6491	0.9999
0.8	0.65	0.8011	0.6452	0.7965	0.6335	0.7986	0.6493	0.8033	0.6504
0.9	0.8	0.8983	0.8017	0.8878	0.8067	0.8962	0.9997	0.8932	0.7982
0.95	1	0.9477	0.9972	0.9410	0.9998	0.9838	0.9997	0.9391	0.9997

Table 6. Position of the tumor and the output of the ANN for a transmitter antenna at 60°, 75° and 90°.

Real position of the tumor (cm/10)		Output of the ANN (SCG)					
		Antenna at 60°		Antenna at 75°		Antenna at 90°	
X	Y	X	Y	X	Y	X	Y
0	0.9	0.0001	0.8935	0.0006	0.9468	0.0000	0,9109
0.05	0.6	0.0415	0.5997	0.0494	0.5971	0.0466	0.6137
0.1	0.65	0.0944	0.6501	0.0930	0.6587	0.1021	0.6489
0.15	0.85	0.1596	0.8519	0.1302	0.8549	0.1561	0.0852
0.25	0.7	0.2519	0.7005	0.2478	0.6911	0.2477	0.6936
0.25	1	0.2607	0.9987	0.2176	0.9986	0.2766	0.9999
0.45	0.5	0.4501	0.5007	0.4579	0.5015	0.4509	0.501
0.65	1	0.6429	0.9992	0.7069	0.9978	0.8114	1
0.8	0.65	0.7986	0.6489	0.8070	0.6450	0.8047	0.6522
0.9	0.8	0.8964	0.8011	0.8877	0.8022	0.8932	0.8074
0.95	1	0.9597	0.9938	0.9407	0.9612	0.9425	0.9836

Table 7. Position of the tumor and the output of the ANN for a transmitter antenna at 0°, 15°, 30° and 45°.

Real position of the tumor (cm/10)		Output of the ANN (GDM)							
		Antenna at 0°		Antenna at 15°		Antenna at 30°		Antenna at 45°	
X	Y	X	Y	X	Y	X	Y	X	Y
0	0.9	0.0240	0.9101	0.0400	0.8968	0.0243	0.9056	0.0027	0.8745
0.05	0.6	0.0849	0.6046	0.0525	0.6124	0.0384	0.5986	0.0494	0.6075
0.1	0.65	0.0984	0.6339	0.0850	0.7097	0.0935	0.6508	0.1144	0.6529
0.15	0.85	0.0907	0.8447	0.1274	0.7931	0.1353	0.8363	0.1431	0.8558
0.25	0.7	0.2549	0.7019	0.2375	0.7049	0.2503	6.9891	0.2491	0.7027
0.25	1	0.2688	0.9693	0.2895	0.8915	0.2408	0.9943	0.2870	0,9919
0.45	0.5	0.4102	4.9518	0.4452	0.5002	0.4425	0.4980	0.4459	0.5015
0.65	1	0.6561	0.9758	0.6262	0.9194	0.6410	0.9990	0.6518	0.9909
0.8	0.65	0.7969	0.6298	0.8487	0.6752	0.7997	0.6514	0.7926	0.6487
0.9	0.8	0.9034	0.7989	0.8838	0.7656	0.9203	0.8053	0.9028	0.8010
0.95	1	0.9360	0.9757	0.9044	0.9296	0.9462	0.9919	0.9478	0.9836

Table 8. Position of the tumor and the output of the ANN for a transmitter antenna at 60°, 75° and 90°.

Real position of the tumor (cm/10)		Output of the ANN (GDM)					
		Antenna at 60°		Antenna at 75°		Antenna at 90°	
X	Y	X	Y	X	Y	X	Y
0	0.9	0.0234	0.8975	0.0487	0.9248	0.0008	0.8972
0.05	0.6	0.0537	0.6087	0.0789	0.5858	0.0495	0.6057
0.1	0.65	0.0902	0.6403	0.0918	0.6361	0.1042	0.6556
0.15	0.85	0.1320	0.8741	0.1357	0.8649	0.1510	0.8569
0.25	0.7	0.2555	0.7017	0.2254	0.7289	0.2444	0.6923
0.25	1	0.2510	0.9685	0.2245	0.2245	0.2458	0.9974
0.45	0.5	0.4558	0.5103	0.4517	0.4972	0.4491	0.5035
0.65	1	0.6304	0.9590	0.6709	0.9293	0.6617	0.9917
0.8	0.65	0.8021	0.6238	0.8546	0.7280	0.7894	0.6588
0.9	0.8	0.9043	0.8142	0.8912	0.8158	0.9216	0.8048
0.95	1	0.9234	0.9586	0.8305	0.8728	0.9379	0.9742

Table 9. Recognition rate and relative error for each antenna.

Location of antenna	Recognition rate (%)		Relative error (%)	
	Trainscg	Traingdm	Trainscg	Traingdm
Antenna at 0°	89	84	1.13×10^{-5}	0.00971
Antenna at 15°	92	81	1.00×10^{-6}	0.000951
Antenna at 30°	97	96	1.00×10^{-6}	0.00182
Antenna at 45°	99	97	1.00×10^{-6}	0.000464
Antenna at 60°	100	95	1.00×10^{-6}	0.000228
Antenna at 75°	96	78	1.89×10^{-6}	0.00141
Antenna at 90°	88	88	1.00×10^{-6}	0.000692

4. DISCUSSIONS

The detection of the tumor by a neural network have been studied for several locations of the transmitter antenna from 0° to 90° with a step of 15° (Fig. 2). Two algorithms have been used for the learning of each neural network trainscg and traingdm (see Tables 5–8). The positions obtained at the output of the ANN for each antenna location are very close to the real position under CST except for some of them that are relatively far as shown in Tables 5–8.

From Table 9, it is noted that for an antenna placed at 60° (Fig. 2) the best recognition rate is obtained with trainscg which is 100%, whereas the antenna locations obtained are, respectively, at 45° giving a rate of 99%, at 30° with a rate of 97%, at 75° with a rate of 96%, at 15° with a rate of 92%, at 0° with a rate of 89%, and finally a rate of 88% is noted for the antenna placed at 90° (Fig. 2).

The fact of making a rotation of the emitting antenna (Fig. 2) throughout the breast ensures a higher detection rate because with a single antenna position (antenna at 0°) case studied in [16] there is a great risk that the tumor is not placed in the radiation field of the transmitting antenna at this emplacement, and therefore, there will be no detection. It is also noticed that the learning algorithm trainscg gives a better result than traingdm.

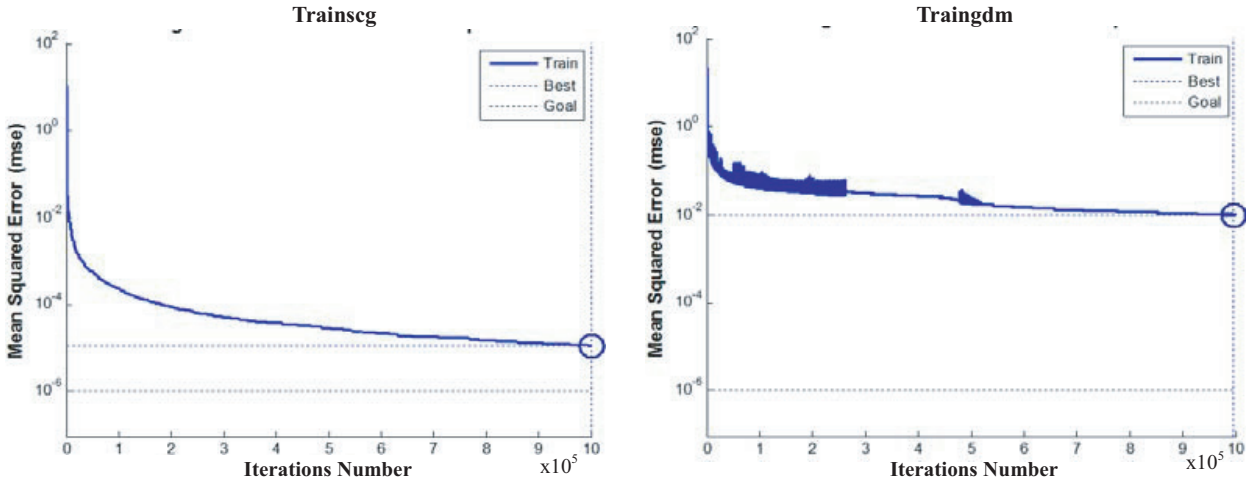

Figure 5. Performance of the learning phase for trainscg and traingdm for an antenna at 0°.

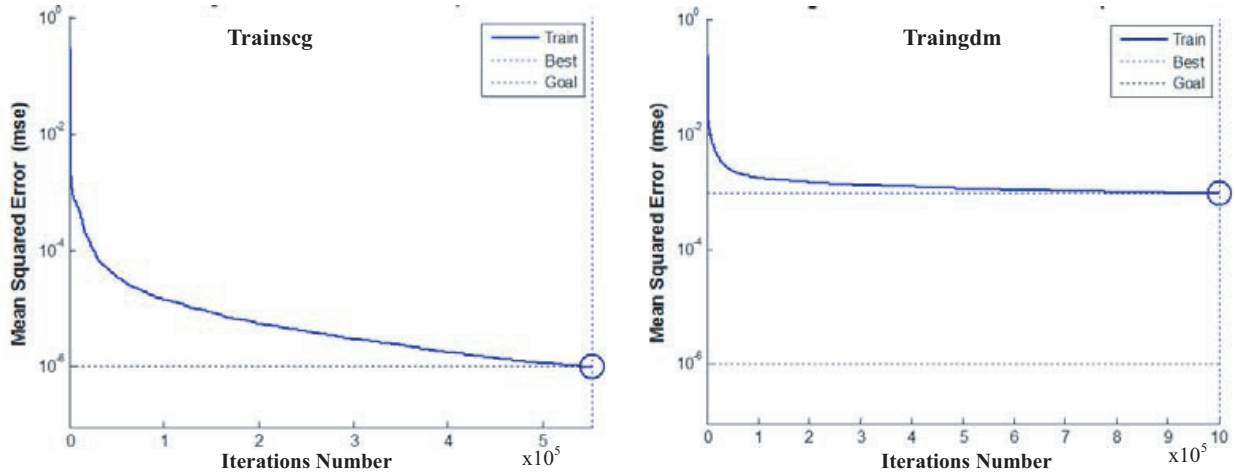

Figure 6. Performance of the learning phase for trainscg and traingdm for an antenna at 15°.

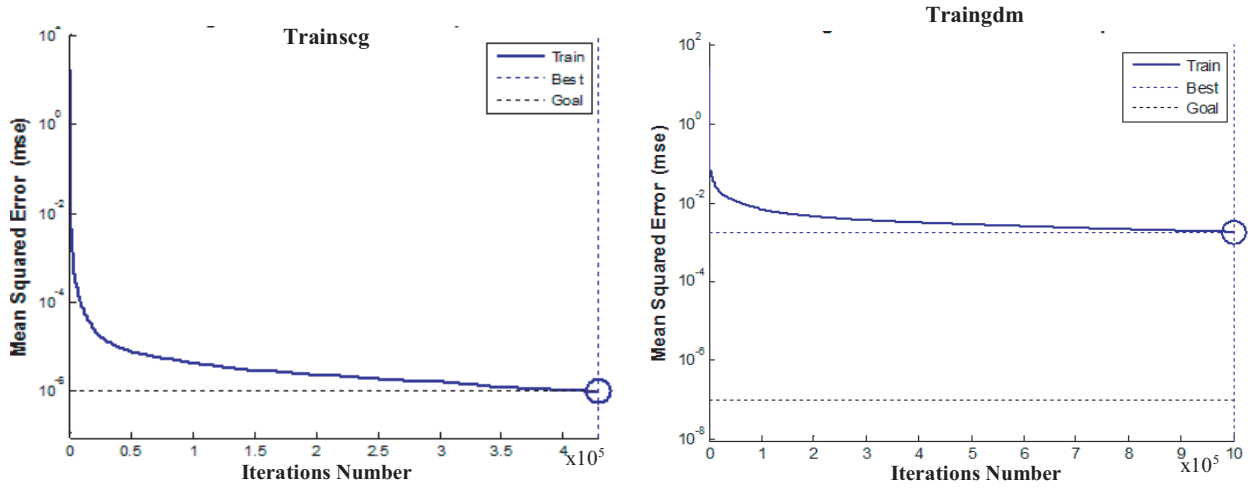

Figure 7. Performance of the learning phase for trainscg and traingdm for an antenna at 30°.

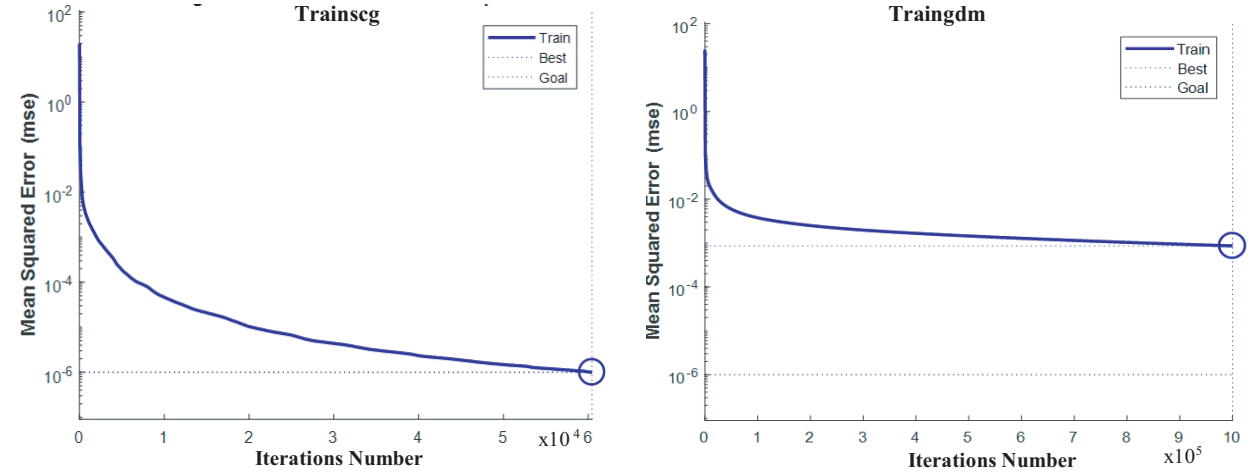

Figure 8. Performance of the learning phase for trainscg and traingdm for an antenna at 45°.

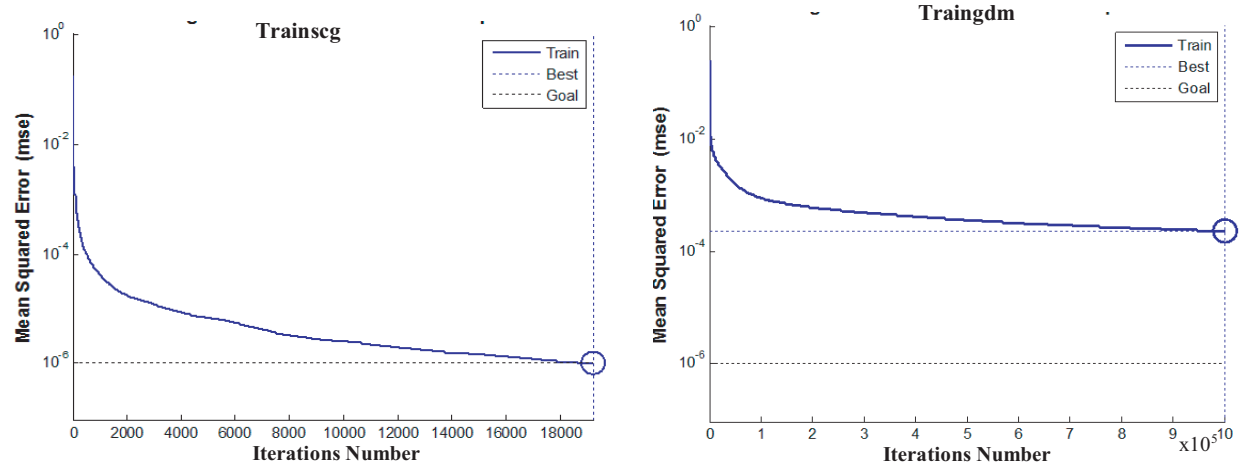

Figure 9. Performance of the learning phase for trainscg and traingdm for an antenna at 60°.

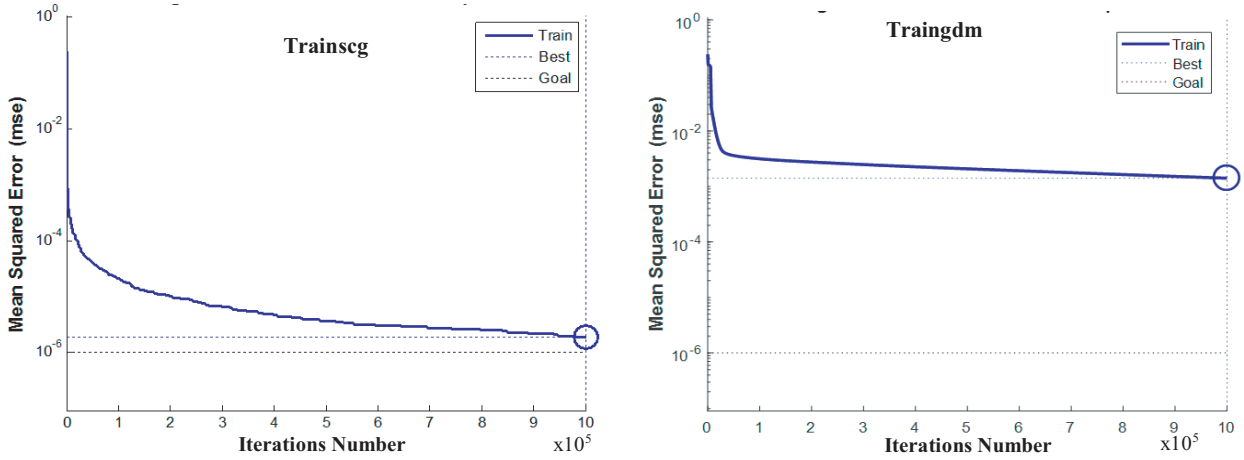

Figure 10. Performance of the learning phase for trainscg and traingdm for an antenna at 75°.

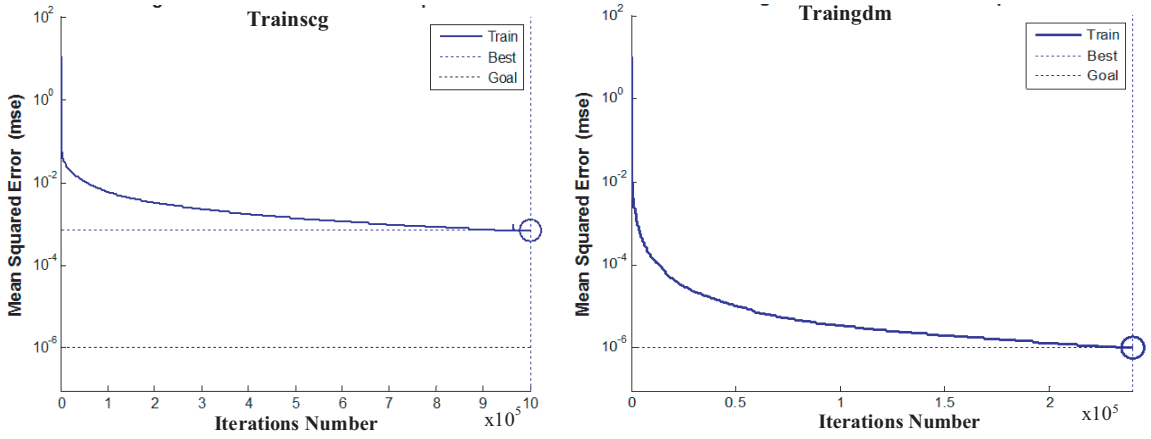

Figure 11. Performance of the learning phase for trainscg and traingdm for an antenna at 90°.

5. CONCLUSIONS

In this work, a comparative study is conducted for the detection of breast cancer by an artificial neural network using two learning algorithms trainscg and traingdm. This is done by rotating the transmitter antenna on different locations from 0° to 90° with step of 15°. The learning algorithm trainscg gives better results than traingdm for the detection of tumor for each antenna location. These simulation results are very satisfactory in terms of detection.

This method gives an optimal recognition rate for different locations of the transmitting antenna around the breast (60°, 45°, 30°, 75°) as shown in Table 9. So it is appreciated that it is a promising technique for detection of the tumor at any location in the breast. As perspectives, it is suggested to treat a similar study by decreasing the rotation step of the transmitting antenna. Also, it is interesting to look for a detection and localization of a tumor object in 3D. Finally, a study of a heterogeneous breast prototype is recommended.

REFERENCES

1. Conceic*a*o, R. C., M. O'Halloran, M. Glavin, and E. Jones, "Numerical modelling for ultra wideband radar breast cancer detection and classification," *Progress In Electromagnetics Research B*, Vol. 34, 145–171, 2011.

2. Fear, E. C., S. C. Hagness, P. M. Meany, M. Okoniewski, and A. Stuchlym, "Enhancing breast tumor detection with near field imaging," *IEEE Microwave Magazine*, Vol. 3, 48–56, 2002.
3. Elmore, J. G., M. B. Barton, V. M. Moceri, S. Polk, P. J. Arena, and S. W. Fletcher, "Ten year risk of false positive screening mammography and clinical breast examinations," *New England Journal of Medicine*, Vol. 338, 1089–1096, 1998.
4. Li, X. and S. C. Hagness, "A confocal microwave imaging algorithm for breast cancer detection," *IEEE Microwave and Wireless Components Letters*, Vol. 11, No. 3, March 2001.
5. AlShehri, S. A. and S. Khatun, "UWB imaging for breast cancer detection using neural network," *Progress In Electromagnetics Research C*, Vol. 7, 79–93, 2009.
6. Fear, E. C. and M. A. Stuchly, "Microwave detection of breast cancer," *IEEE Transactions on Microwave Theory and Techniques*, Vol. 48, 1854–1863, 2000.
7. Chaudhary, S. S., R. K. Mishra, A. Swarup, and J. M. Thomas, "Dielectric properties of normal and malignant human breast tissues at radiowave and microwave frequencies," *Indian Journal of Biochemistry and Biophysics*, Vol. 21, 76–79, 1981.
8. Alshehri, S. A., "Experimental breast tumor detection using NN-based UWB imaging," *Progress In Electromagnetics Research*, Vol. 111, 447–465, 2011.
9. Alshehri, S. A., "3D experimental detection and discrimination of malignant and benign breast tumor using NN-based UWB imaging," *Progress In Electromagnetics Research*, Vol. 116, 221–237, 2011.
10. O'Halloran, M., B. McGinley, R. C. Conceicao, F. Morgan, E. Jones, and M. Glavin, "Spiking neural networks for breast cancer classification in a dielectrically heterogeneous breast," *Progress In Electromagnetics Research*, Vol. 113, 413–428, 2011.
11. Furundzicn, D., M. Djordjevic, and A. J. Bekic, "Neural networks approach to early breast cancer detection," *Journal of Systems Architecture*, Vol. 44, No. 617, 6339, 1998.
12. Bindu, G., A. Lonappan, V. Thomas, C. K. Aanandan, and K. T. Mathew, "Active microwave imaging for breast cancer detection," *Progress In Electromagnetics Research*, Vol. 58, 149–169, 2006.
13. Seladji, N., F. Z. Marouf, L. Merad, S. M. Meriah, F. T. Bendimerad, M. Bousahla, and N. Benahmed, "Antenne microruban miniature ultra large bande ULB pour imagerie microonde," *Proceedings of the Congrès Méditerranéen des Télécommunications (CMT'12)*, 21–25, Fès, Morocco, March 22–24, 2012.
14. Miyakawa, M., T. Ishida, and M. Wantanabe, "Imaging capability of an early stage breast tumor by CP-MCT," *Proceedings of the 26th Annual International Conference of the IEEE EMBS*, Vol. 1, 1427–1430, San Francisco, CA, USA, 2004.
15. Miraoui, A., L. Merad, and S. M. Meriah, "Breast tumor classification using support vector machine and artificial neural networks," *International Journal of Microwave and Optical Technology*, Vol. 12, No. 2, March 2017.
16. Miraoui, A., L. Merad, and S. M. Meriah, "Microwave imaging for the detection and localization of breast cancer using artificial neural network," *Journal of Theoretical and Applied Information Technology*, Vol. 74, No. 3, April 30, 2015.